

Noninvasive nature of corona charging on thermal Si/SiO₂ structures

M. S. Dautrich, P. M. Lenahan, A. Y. Kang, and J. F. Conley Jr.

Citation: *Applied Physics Letters* **85**, 1844 (2004); doi: 10.1063/1.1789576

View online: <http://dx.doi.org/10.1063/1.1789576>

View Table of Contents: <http://scitation.aip.org/content/aip/journal/apl/85/10?ver=pdfcov>

Published by the AIP Publishing

Articles you may be interested in

Paramagnetic point defects in (100) Si/LaAlO₃ structures: Nature and stability of the interface

J. Appl. Phys. **102**, 034516 (2007); 10.1063/1.2749423

Invasive nature of corona charging on thermal Si/SiO₂ structures with nanometer-thick oxides revealed by electron spin resonance

Appl. Phys. Lett. **82**, 2835 (2003); 10.1063/1.1540245

Thermally induced interface degradation in (100) and (111) Si/SiO₂ analyzed by electron spin resonance

J. Vac. Sci. Technol. B **16**, 3108 (1998); 10.1116/1.590449

Hydrogen-induced thermal interface degradation in (111) Si/SiO₂ revealed by electron-spin resonance

Appl. Phys. Lett. **72**, 2271 (1998); 10.1063/1.121335

Electron spin resonance features of interface defects in thermal (100) Si/SiO₂

J. Appl. Phys. **83**, 2449 (1998); 10.1063/1.367005



Noninvasive nature of corona charging on thermal Si/SiO₂ structures

M. S. Dautrich,^{a)} P. M. Lenahan, and A. Y. Kang
 Pennsylvania State University, University Park, Pennsylvania 16802

J. F. Conley, Jr.
 Sharp Labs of America, Camas, Washington 98607

(Received 10 March 2004; accepted 7 July 2004)

The corona charging technique is widely utilized in commercial Si/SiO₂ semiconductor device reliability characterization tools and has been used in numerous electron spin resonance (ESR) experiments, by several groups to study defect centers in Si/SiO₂ system. A recent ESR study argued that the corona charging approaches are inherently unreliable and invasive. In this work we show that this is not the case. We find that low-field corona biasing is essentially noninvasive and thus can be utilized in both reliability characterization and fundamental studies of defect structures. © 2004 American Institute of Physics. [DOI: 10.1063/1.1789576]

Comparatively low-field corona biasing is an essential part of several widely utilized commercial device reliability characterization tools. Examples include the Quantox systems of KLA-Tencor¹ and the Corona Oxide Characterization of Semiconductor (COCOS) technology of Semiconductor Diagnostics.² In several early studies involving electron spin resonance (ESR),^{3–7} low-field corona biasing was utilized to manipulate the position of the Fermi energy at the Si/SiO₂ boundary, providing information about the density of states of Si/SiO₂ interface trapping centers. In all of these cases, the validity of the measurements requires that little or no relevant damage occurs to the Si/SiO₂ system as a result of the biasing. Other early ESR studies,^{8,9} utilizing quite high field corona bias, demonstrated that high oxide field corona biasing can clearly generate both large densities of Si/SiO₂ interface and oxide paramagnetic centers.

Recently, Stesmans and Afanas'ev¹⁰ have argued that corona charging techniques are “inherently unreliable” and that, when applied to thin oxides on silicon, the technique is invasive and “intolerably modifies the inherent properties of the entity studied, leaving it quite disrupted in terms of (ESR-active) defects.” They argued that earlier ESR studies done at low-field^{3–7,11} and the commercial device characterization tools are unreliable.

In our study, we compare the response of oxide films to both high and somewhat lower field corona bias for both thick and thin film samples. Our results demonstrate quite clearly that distinctions must be made between low- and high-field corona charging. We find that low-field corona charging appears to be relatively harmless, whereas high-field corona-charging, as earlier studies^{8,9} have also shown, is quite damaging. Our results clearly support both the usefulness of the corona biasing reliability tools and the validity of earlier low-field corona ESR studies.

Our measurements utilized 75 and 634 Å SiO₂ films thermally grown in dry oxygen on relatively high (350–500 Ω cm) resistivity *n*-type silicon substrates with (111) surface orientation. The (111) orientation was chosen to simplify the ESR analysis. All wafers received a postdeposition anneal in forming gas (N₂/H₂) at 400 °C for 30 min and were cleaned using a standard SC1/SC2/HF process

prior to oxidation. Room temperature magnetic resonance measurements were made at X band with a commercial state-of-the-art ESR spectrometer (Bruker Instruments) using a TE₁₀₄ double cavity and a weak pitch spin standard. Corona biasing followed the scheme described by Weinberg *et al.*¹² Low-field oxide bias was measured using a Kelvin probe. We subjected devices to up to 20 h of corona biasing at various oxide potentials, periodically making ESR measurements of the oxide/silicon structures. The oxides were stressed with the Si surface (*n*-type) in accumulation.

Figure 1 illustrates ESR traces taken on the thick (634 Å) oxides subjected to either high-field (+7 MV/cm) or lower-field (+4 MV/cm) corona biasing (a trace of an unstressed sample has been included for reference). The high-field stressed sample exhibited large numbers ($\approx 4.5 \times 10^{11}/\text{cm}^2$) of P_b and E' centers. In the samples subjected to equal periods of lower field corona biasing, we observed near negligible ($< 3 \times 10^{10}/\text{cm}^2$, about our sensitivity limit in this study) numbers of paramagnetic centers. The low-field stressing defect density is, within experimental error, the same as that of the unstressed sample. In Fig. 2, we plot the change in P_b density (ΔP_b) as a function of corona biasing time for both high and lower values of corona bias on the thick oxides.

In stressing thin (75 Å) oxides we selected +6.5 MV/cm for our high-field and +4 MV/cm as well as +1 MV/cm for

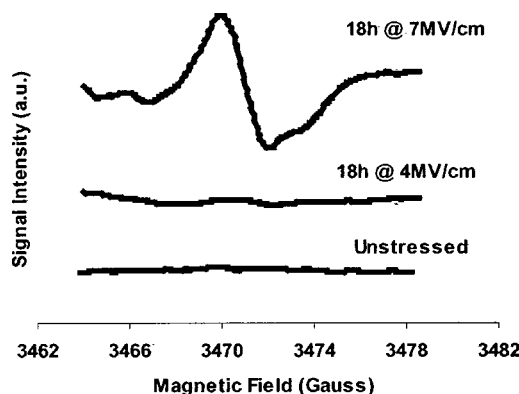


FIG. 1. Pre- and post-corona bias ESR trace on thick (634 Å) oxides with unstressed trace as reference. The slight asymmetry in the high-field trace is due to weak generation of E' centers.

^{a)}Electronic mail: msd153@psu.edu

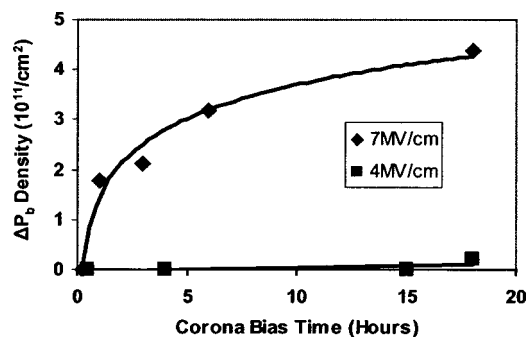


FIG. 2. Comparison of high (+7 MV/cm) and lower (+4 MV/cm) corona biasing time vs defect generation on thick (634 Å) oxides. Note: near negligible P_b center generation occurs in the lower corona bias samples.

our low-field corona biasing. As was the case for thicker oxides, the high-field stressed sample exhibited generation of very large densities ($\approx 2.1 \times 10^{12}/\text{cm}^2$) of P_b and E' centers whereas the low-field stressed samples showed negligible generation of centers (pre- and post-stressed samples both exhibited $\approx 2 \times 10^{11}$ spins/ cm^2). Figure 3 depicts the change in P_b density in thin samples as a function of stressing time. Note that the oscillatory pattern is not experimental error and indicates competition between the P_b and E' centers. This is consistent with the model proposed by Lenahan and Conley,^{13–16} which involves the minimization of Gibbs free energy of two systems of silicon dangling bonds with hydrogen passivation. The creation of oxide silicon dangling bond defects, E' centers, unpassivated by hydrogen, in the presence of a high density of Si/SiO₂ interface silicon dangling bonds, passivated by hydrogen, creates a situation in which the system's Gibbs free energy may be lowered by transferring hydrogen from one type of site (hydrogen passivated P_b centers) to another (unpassivated oxide E' centers).^{13–16} Depending upon the balance between the passivated E' and P_b centers, the reaction may be driven either way, toward more passivated P_b centers or more passivated E' centers.^{13–16}

Additional wider magnetic field ESR scans of our high field (6.5 MV/cm) thin oxide (not shown) also indicate several defect centers including the generation of E' , P_b , and possibly the nonbridging oxygen defect.

Our results clearly demonstrate that, whereas the higher field corona bias (6.5 MV/cm) generates large numbers of

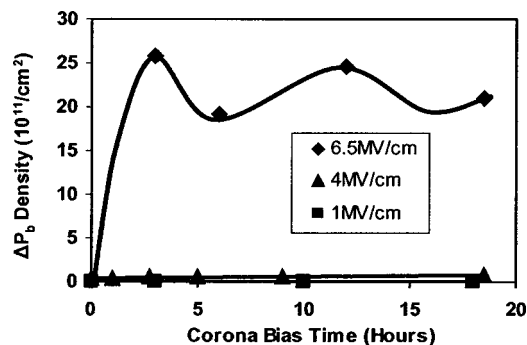


FIG. 3. Comparison of high (+6.5 MV/cm), low (+4 MV/cm), and very low (+1 MV/cm) corona biasing time vs defect generation on thin (75 Å) oxides. Note that as mentioned in the text, the oscillating behavior is almost certainly not experimental error, but the result of a competition between the P_b and E' sites for hydrogen.

defects, the somewhat lower field corona biasing (≤ 4 MV/cm) provides a relatively noninvasive means of applying oxide bias. The results strongly indicate that the much lower corona fields (≤ 2 MV/cm) utilized in reliability tools and in the earlier low-field corona biasing ESR studies^{3–7,11} had no damaging effect. More precisely, with sensitivity threshold of about 3×10^{10} paramagnetic defects/ cm^2 , we observe no defect generation in samples stressed at low-field corona bias. Since this baseline is below the sensitivity limit of the earlier low-field corona biasing ESR studies^{3–7} and the same order of magnitude as the defect density level in device quality interfaces, we conclude that little or no *relevant* damage occurs to the Si/SiO₂ system as a result of this low-field corona biasing. (It should probably be noted that our results may or may not be relevant to *extremely* thin oxides since our investigation involved oxides no thinner than 75 Å).

Additionally we find that the overall response to corona bias is essentially the same in both our thick and thin oxides: high fields are damaging and low fields are not. Our results also support earlier studies^{8,9} which showed that high electric fields generated by corona ions are similar to high electric fields generated by more conventional means, in that both damage the oxides. In fact, as earlier studies have argued,^{8,9} high-field stressing via corona biasing may be at least very roughly equivalent to high-field stressing via conventional gate biasing. However, at lower fields, corona biasing, as conventional biasing causes negligible damage. Thus a distinction must be made between high- and low-field corona biasing.

We find that whereas high-field corona bias induces large densities of paramagnetic centers, lower-field corona biasing generates virtually none. Our results thus support the validity of the earlier low-field corona bias work. Our results also indicate that commercial oxide characterization tools based on the corona principle are not compromised by shortcomings inherent in the technique. We find that corona biasing, as does conventional gate biasing, causes negligible damage at low fields, but generates numerous defects at high fields.

¹KLA-Tencor (Milpitas, CA 95035) manufactures an in-line monitoring and characterization tool called Quantox XP (<http://www.kla-tencor.com/>).

²M. Wilson, J. Lagowski, A. Savtchouk, L. Jastrzebski, and J. D'Amico, ASTM Conference on Gate Dielectric Oxide Integrity, San Jose, CA, 1999.

³P. M. Lenahan and P. V. Dressendorfer, J. Appl. Phys. **55**, 3495 (1984).

⁴P. M. Lenahan and P. V. Dressendorfer, Appl. Phys. Lett. **41**, 542 (1982).

⁵P. M. Lenahan and P. V. Dressendorfer, J. Appl. Phys. **54**, 1457 (1983).

⁶Y. Y. Kim and P. M. Lenahan, J. Appl. Phys. **64**, 3551 (1988).

⁷G. J. Gerardi, E. H. Poindexter, and P. J. Caplan, Appl. Phys. Lett. **49**, 348 (1986).

⁸W. L. Warren and P. M. Lenahan, Appl. Phys. Lett. **49**, 1296 (1986).

⁹W. L. Warren and P. M. Lenahan, IEEE Trans. Nucl. Sci. **34**, 1355 (1987).

¹⁰A. Stesmans and V. V. Afanas'ev, Appl. Phys. Lett. **82**, 2835 (2003).

¹¹J. P. Campbell and P. M. Lenahan, Appl. Phys. Lett. **80**, 1945 (2002).

¹²Z. A. Weinberg, W. C. Johnson, and M. A. Lampert, J. Appl. Phys. **47**, 248 (1976).

¹³P. M. Lenahan, J. F. Conley, Jr., and B. D. Wallace, J. Appl. Phys. **81**, 6822 (1997).

¹⁴J. F. Conley, Jr., P. M. Lenahan, B. D. Wallace, and P. Cole, IEEE Trans. Nucl. Sci. **44**, 1804 (1997).

¹⁵P. M. Lenahan and J. F. Conley, Jr., Appl. Phys. Lett. **71**, 3126 (1997).

¹⁶P. M. Lenahan, J. J. Mele, J. F. Conley, Jr., R. K. Lowry, and D. Woodbury, IEEE Trans. Nucl. Sci. **46**, 1534 (1999).